photonics

MDPI

Article

Simplified Laser Frequency Noise Measurement Using the Delayed Self-Heterodyne Method

Seán P. Ó Dúill * and Liam P. Barry

Radio and Optics Communication Laboratory, School of Electronic Engineering, Dublin City University, D09 V209 Dublin, Ireland; liam.barry@dcu.ie

* Correspondence: sean.oduill@dcu.ie

Abstract: Here, we report on a simplified laser frequency noise measurement technique employing an acousto-optic modulator, a delay line, and a real-time oscilloscope. The technique is a slight modification of the typical delayed heterodyne method. Instead of using a swept frequency spectrum to analyze the laser emission spectrum, the waveform captured on a real-time oscilloscope is used to directly calculate the laser frequency noise. The oscilloscope bandwidth and sampling requirements can be kept modest by choosing a modulator driven at a few hundred megahertz, making this technique attractive for a large number of laboratories. We show the frequency noise measurements of two different lasers with linewidths at 2.7 kHz and 2 MHz. We took the opportunity to investigate the noise floor of the frequency noise measurement system, and we found that the noise floor of the frequency noise measurement depends on the power level of the laser that is being characterized, with the kilohertz linewidths laser requiring more power to reduce the noise floor to acceptable levels.

Keywords: optical metrology; laser linewidth; phase noise; signal processing

Citation: Dúill, S.P.Ó.; Barry, L.P. Simplified Laser Frequency Noise Measurement Using the Delayed Self-Heterodyne Method. *Photonics* **2024**, *11*, 813. https://doi.org/10.3390/photonics11090813

Received: 11 July 2024
Revised: 23 August 2024
Accepted: 28 August 2024
Published: 29 August 2024

1. Introduction

Laser phase noise is a key metric in determining the quality of the laser source and for identifying potential applications for the source, e.g., optical communications, time keeping, and LIDAR, to name a few [1–6]. Ideally, a laser will possess Lorentzian-shaped line broadening, owing to the spontaneous emission in the laser cavity [7]. A recent tutorial paper collating the early works on laser line broadening is given in [8]. Laser linewidth is typically measured using the delayed self-heterodyne (DSH) method [9–13], where a frequency-shifted copy of the laser light is beat with a delayed copy of the laser light at a photodetector. The linewidth is then extracted by fitting the swept spectrum measurement of the beat frequency to a Voigt curve [14], which is a Lorentzian-shaped curve (representing the intrinsic Lorentzian linewidth) convolved with a Gaussian-shaped curve (representing the slow wavelength drift). We refer to the swept frequency method as the DSH method, since this term is well known for the description of this scheme [11,12]. The Gaussian part of the beat spectrum is caused by the slow wavelength drift of the laser on timescales typically longer than 1 µs. While the intrinsic linewidth is of importance for optical communications, newer laser applications, such as LIDAR, require knowledge of the slower wavelength drift, including not only the magnitude, but also the timescales at which the slow wavelength drift become significant [1,15].

The frequency noise (FN) spectrum is an alternative measurement to the DSH method [16]. The main benefit of the FN spectrum is that the technique completely decouples the intrinsic Lorentzian linewidth measurement from the slower wavelength drift. The slower wavelength drift appears as $1/f$ shape in the FN spectrum [16,17]. The FN spectrum is related to the DSH spectrum, and a Lorentzian-line-broadened laser possesses a flat FN spectrum; in addition, the relationships between the DSH and FN spectrum measurements are given in [16]. Another major benefit of measuring the FN spectrum over the DSH spectrum is

that the laser linewidth does not limit the minimum intrinsic Lorentzian linewidth that can be measured [18], which unfortunately is the case for the DSH method [12], i.e., the fiber delay line does not have to be longer than the coherence time of the laser (related to the inverse of the linewidth). We have proposed methods to measure the FN spectrum, as follows: (i) through a phase-modulation (PM) method [17] and (ii) through a frequency-shift method [18]. The PM technique requires strong phase modulation to suppress the optical carrier, as well as digital demodulation of two beat tones and significant digital signal processing, especially implementing linear phase digital low pass filters, for that scheme to work. In the frequency-shift method outlined in [18], we showed a cumbersome frequency-shifting technique used to measure the FN spectrum without the need for complex digital signal processing. The RF detection used Inphase-Quadrature demodulation within an electrical spectrum analyzer (ESA); therefore, the cost of such instrumentation limits the wide deployment of that technique. However, the main goal of that work was to prove the ability of the FN method to measure linewidths of the order of 10 Hz with fiber delay lines shorter than the laser coherence time; moreover, we were also able to understand the limitation that the fiber delay line imposes on calculating the FN spectrum.

In this paper, we propose a vastly simplified FN spectrum measurement technique based on the DSH method using an acousto-optical modulator (AOM) as the frequency-shifting element and a real-time oscilloscope (RTO) with modest specifications to measure the beat tone created in a photodiode. AOMs are standard fare in DSH systems. Typically, in a DSH system [9–12], an ESA is used to sweep across the beat signal and measure the spectrum. In this work, we substitute an RTO for an ESA, allowing us to measure the FN spectrum without any other changes to the hardware setup. The scheme relies on applying a single-sideband frequency-shift element and processing the beat frequency component at the photodiode, as for a two-laser heterodyne system [19]. The RTO requirements in terms of bandwidth are proportional to the AOM modulating frequency, which is a few hundred megahertz. The FN spectrum is calculated for two different lasers, including one laser that has a very narrow linewidth of 2.7 kHz, while the other laser has a linewidth of about 2 MHz. This covers the typical range of laser linewidths that one would encounter for a large range of applications. We found that the linewidth values agree with the extracted value from the traditional DSH method with Voigt lineshape fitting [14]. We were further able to corroborate the FN results for the narrow linewidth laser by measuring the phase noise analysis (PNA) spectrum of the beat tone using an ESA [20]. In this work, we took the opportunity to investigate the noise floor of the FN measurement and found that the noise floor of the measurement increases when the received power is reduced, and the emergence of the noise floor affects lasers with smaller linewidths below, say, 10 kHz. Even though we highlight the scheme for lasers operating at 1300 nm, there is no restriction on the operating wavelength, provided a suitable frequency shifter is available at those wavelengths. The paper is organized as follows: first, we outline the technique and describe the digital processing steps used to extract the FN spectrum, then the FN spectra for two different lasers are presented along with the verifying DSH spectra.

2. Materials and Methods

The DSH setup is shown in Figure 1. Light from a continuous wave (CW) laser is split in two arms, as follows: on the upper arm, the light is frequency shifted by the modulating frequency f_m of an AOM; the light in the lower arm is delayed in a fiber delay line with delay τ; and the length of the fiber used is 4.8 km. The light from both arms is then recombined and an electrical RF beat-component centered at f_m is generated at the photodiode and amplified in a transimpedance amplifier. The RF voltage is then sampled using an RTO with a 300 MHz analogue bandwidth, a sampling rate of 2.5 GSa/s, 10-bit sampling resolution, and a memory depth of 5 MSa. The beat component can also be analyzed using an electrical spectrum analyzer to look at the averaged DSH spectrum of the beat frequency or using the PNA tool in an ESA.

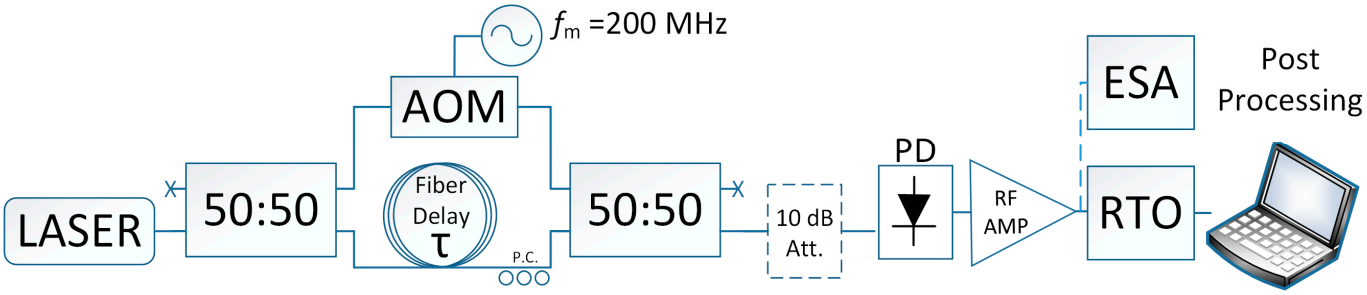

Figure 1. FN measurement setup. Light from a CW laser is split between two paths: one path is frequency shifted by 200 MHz using the AOM, while the other path is delayed by a length of optical fiber. Light from the two paths is recombined and mixed in the photodiode, creating a beat component centered at 200 MHz. The RTO samples the beat signal, and offline post-processing extracts the FN. The beat signal can also be analyzed using the ESA with the (i) traditional swept spectrum technique or (ii) using the PNA functional to detect the phase noise spectrum at 200 MHz. The placement of a 10 dB attenuator (10 dB Att.) is shown for the investigation of reducing the optical power and is not normally necessary for the scheme to work. A polarization controller (P.C.) is used to maximize the strength of the beat signal at the photodetector. Dotted lines indicate secondary measurement conducted within this study, though is not necessary to the FN measurement. An 'X' denotes a fibre termination or unused port from an optical coupler.

The most appropriate device to use to perform frequency shifting is the AOM. The averaged spectrum DSH measurement is possible to obtain irrespective of whether an electro-optic PM or AOM is used, though we will show why the FM noise measurement is much simplified when an AOM is used instead of a PM. In the AOM case, the beating between the light from both arms resembles that of heterodyning two separate lasers with the beat tone centered at the modulating frequency of f_m with constant amplitude sinewave and the phase noise encoded in the phase of the beat sinewave. The phase noise can be extracted using techniques applicable to two laser heterodyning [19]. The beat signal is captured using an RTO with an analog bandwidth of at least ~$2f_m$ and, thus, a sampling rate of at least $4f_m$. The value of f_m throughout this work is 200 MHz. The reason why using a frequency shifter is simpler than the PM method is because, for the frequency-shift method, as previously mentioned above, the amplitude of the beat component at the fundamental is constant; however, for the PM method, the amplitudes of the fundamental and first harmonic of the beat tones are intensity modulated by the sine and cosine of the phase noise, respectively, thus requiring both terms to be captured. The full analysis outlining the PM method is given in [17], including all of the signal processing steps.

The detected photocurrent at the beat frequency from the photodiode in Figure 1 is given by the following:

$$I_{pd} = rE_{AOM}E_{FD}\cos[(2\pi f_m t + \theta(t) - \theta(t-\tau))] \quad (1)$$

where r is the photodiode responsivity, E_{AOM} describes the amplitude of the optical field after the AOM, E_{FD} describes the amplitude of the optical field after the fiber delay line, τ is the delay of the fiber delay line, and θ is the phase noise laser. For CW lasers with low intensity noise, one can ignore amplitude fluctuations in I_{PD}. The detected voltage with the RTO is proportional to (1), which is a sinewave voltage oscillating at f_m that incorporates the phase noise $\theta(t) - \theta(t-\tau)$. The quantity of interest when resolving the FN is $\theta(t) - \theta(t-\tau)$ and is extracted as per the basic technique for analyzing a two-laser heterodyne [18,19]. Taking (1) as the In-phase (I) term, the Quadrature term (Q) proportional to $\sin[(2\pi f_m t + \theta(t) - \theta(t-\tau))]$ is obtained by taking the Hilbert transform of (1), i.e., $Q = H[I(t)]$. Therefore, the phase noise term $\vartheta(t) = \theta(t) - \theta(t-\tau)$ is given by the following:

$$2\pi f_m t + \vartheta(t) = \tan^{-1}[I(t), Q(t)] \quad (2)$$

where $\tan^{-1}(I, Q)$ is the two-argument inverse tangent function for phase retrieval over the entire $[-\pi, \pi]$ interval; $2\pi f_m t$ is eliminated by subtracting the linear trend from $\tan^{-1}(I, Q)$ (in practice, this is performed by applying a numerical linear 'detrend' function to $\tan^{-1}(I, Q)$); and the remaining data represent $\vartheta(t)$. The instantaneous frequency is the scaled time derivative.

$$f_N(t) = (2\pi)^{-1} d\vartheta(t)/dt \tag{3}$$

The spectral density of $f_N(t)$ is then calculated and presented as the quality metric of the laser and can be readily calculated using Welch's spectral density estimate [21]. Apart from the captured waveform on the RTO, the only other input to the Welch estimator is the RTO sampling rate and the number of samples in the subset waveforms (much less than the total number of obtained waveform samples) used to evaluate the spectrum in Welch's method. Some care is needed to select the number of samples in the spectral density estimate, because the fiber delay imposes the minimum frequency at which an FN spectral density estimate can be achieved without causing comb-like spectral artifacts in the FN spectrum arising from correlated phase noise terms within each subset waveform. We studied this extensively in [18]. Since the delay line is 4.8 km long, the duration of the subset waveforms when evaluating the spectrum in Welch's method must be shorter than the fiber delay (24 μs) to ensure uncorrelated phase noise terms. Given the sampling rate of 2.5 GSa/s, the maximum number of samples in each subset waveform must be less than 60,000 samples to ensure an uncorrelated phase over every subset waveform. We chose 10,000 samples for each smaller partition from the entire 5 MSa block to calculate the spectrum; moreover, given the sampling rate of 2.5 GSa/s, choosing 10,000 samples allows for >500 spectral averages, which eliminates the uncertainty in the FN spectrum [18]. Note that only the positive half of the FN spectrum is presented over the Fourier frequency range from 250 kHz (2.5×10^9/10,000) to f_m, which is 200 MHz. A sample computer code is written in Appendix A, which is used to extract the FN spectral density from the measured RTO waveform.

Some consideration has to be made when choosing the length of fiber in the delay line. The fiber delay sets the lowest Fourier frequency possible before comb-like effects spoil the FN measurement [18], with the inverse of the fiber delay being the lowest Fourier frequency. In this case, 24 μs imposes the lowest possible Fourier frequency as 41.667 kHz. Increasing the fiber delay lowers the minimum Fourier frequency, though increasing the fiber length also increases the loss, which may hamper the FN measurement.

We also present some corroborating results to validate the FN measurement technique by taking measurements from an ESA. Traditionally, the averaged beat spectrum is measured on an ESA with the intrinsic linewidth extracted by fitting the spectrum to a Voigt lineshape [14]. We perform this measurement to compare with the measured FN curves. Moreover, as an additional check, some ESAs possess a PNA tool to measure the phase noise spectrum of a specified frequency. The relationship between the phase noise spectrum L_φ and the FN spectrum is defined by the following [22]:

$$F_N(f_F) = L_\varphi(f_F) f_F^2 \tag{4}$$

To avoid ambiguity in the definition of frequency to denote the independent variable of F_N or L_φ, the independent for variable is termed Fourier frequency and denoted as:, f_F. For large fiber delays, which we are using in this paper, the slow laser wavelength drift spoils the PNA measurement, though we were able to measure the phase noise spectrum of f_m over the range of Fourier frequencies from 10 MHz to 100 MHz for one laser that had good wavelength stability. The PNA method can work successfully for any laser, provided the delay line is short enough, typically in the order of a few tens of nanoseconds (i.e., length of the fiber-coupled AOM and a polarization controller). The full details of this are given in [21].

Before presenting the results, we highlight the important factors of the FN spectrum. Firstly, for a source with a Lorentzian lineshape, the relationship between the linewidth

(Δf_{3dB}) and the FN means that FN spectral density has a constant value [16] with the following relationship:

$$\Delta f_{3dB} = 2\pi F_N$$

For double-sided FN spectra, the following applies: We scale the FN curves by 2π so that the estimated linewidth values can be directly read from the FN spectra curves. Unless otherwise stated, all FN curves in this paper are scaled FN curves. Since ϑ consists of the subtraction of two random variables that are uncorrelated, due to the long delay line, the actual FN spectral density, PNA spectrum, and extracted Lorentzian linewidths of the lasers are half that of what is calculated; therefore, we halve all of the FN spectra presented in the paper.

In relation to the noise floor of the FN spectral density, this floor is proportional to f_F^2, due to the differential operation shown in Equation (3), and this is evident in measured FN curves [17,18] and most clearly in [23] for fiber lasers with linewidths below 100 Hz.

3. Results

We now present the FN results for two lasers, as follows: one laser, termed henceforth as Laser A, is Littrow-style tunable laser, and this laser was tuned to 1300 nm with 10 dBm fiber-coupled power. As we will show, this laser has an intrinsic Lorentzian linewidth of about 2.7 kHz, thus highlighting the capabilities of this scheme to measure very low linewidths. The other laser, termed henceforth as Laser B, is a DFB laser operating at 1305 nm; furthermore, the bias current for Laser B is 50 mA, yielding a fiber-coupled CW power of 10 dBm. For each laser, we calculate the FN for the following detection scenarios: (i) PiN photodiode followed by an RF transimpedence amplifier with a voltage gain of 10 to boost the beat signal, which considers a typical photodetection scenario. In this case, the typical voltage amplitude was 1.5 V, measured with the RTO, and the RMS noise without light and with the amplifier turned on was 2.1 mV; (ii) PiN alone to see how well the FN measurement performs if a weaker electrical signal is input to the oscilloscope. In this scenario, the voltage amplitude was typically 0.1 V, and the RMS noise detected with the oscilloscope with the light off was 718 μV; (iii) a 10 dB optical attenuator placed before the PiN + RF amplifier to investigate the impact of the CW power from the laser. In this case, the voltage amplitude was typically 0.15 V. The oscilloscope has an analogue bandwidth of 300 MHz, with a sampling rate of 2.5 GSa/s and memory depth of 5 MSa.

The results for Laser A are shown in shown in Figure 2a, where the dark blue curve shows the FN measurement with the PiN + RF Amp scenario. The FN curve is to be interpreted as follows: as mentioned in the introduction, a Lorentzian spectrum implies a constant FN spectrum [16], therefore, the flat portion of the scaled FN curve implies the intrinsic Lorentzian linewidth value. Ignoring the spurious tone at 40 MHz, the flat portion of F_N lies between Fourier frequencies ranging from 10 MHz to 50 MHz, and an intrinsic linewidth of 2.7 kHz is read directly from the scaled FN curve. At lower Fourier frequencies, the increasing FN, with respect to a decreasing Fourier frequency, is related to the slow wavelength drift of the laser. With the PiN alone (red curve), there is little difference between the red and dark blue curves, suggesting that the RF amplifier is not necessary for the measurement. However, when the optical power is attenuated by 10 dB before the PiN, which is shown with the green curve in Figure 2a, the calculated F_N begins to increase with increasing Fourier frequency, according to f_F^2, indicating an elevated noise floor [18]. The noise floor in the FN spectrum increases proportional to f_F^2, due to the differentiation operator when calculating the instantaneous frequency from the instantaneous phase. The emergence of the noise floor for lower power signals is due to the larger (smaller) instantaneous phase shift for weaker (stronger) sinusoidal waves in the presence of additive noise. From this finding, we can conclude that the noise floor of F_N depends on the received optical power, and this becomes important to be aware of, especially when measuring the FN of lasers with very low linewidths of a few kilohertz or smaller. The light blue curve in Figure 2a is taken from the PNA tool within an ESA, modified according to Equation (4), and plotted alongside the FN curves to show agreement

between the two methods. It should be noted that the PNA measurement of the 200 MHz beat tone was only stable for the measurement between Fourier frequencies ranging from 10 MHz to 100 MHz. This is understandable due to the nature of the low frequency laser wavelength drift and the 4.8 km long fiber delay line. The averaged beat spectrum of the beat signal is measured by averaging 100 scans of the swept spectrum on the ESA, and the results are plotted for Laser A in Figure 3a. A Voight curve fit of the beat spectrum was performed, and the intrinsic Lorentzian linewidth component of 2.5 kHz was extracted. The value of 2.5 kHz agrees well with the intrinsic linewidth of 2.7 kHz extracted from the FN measurements.

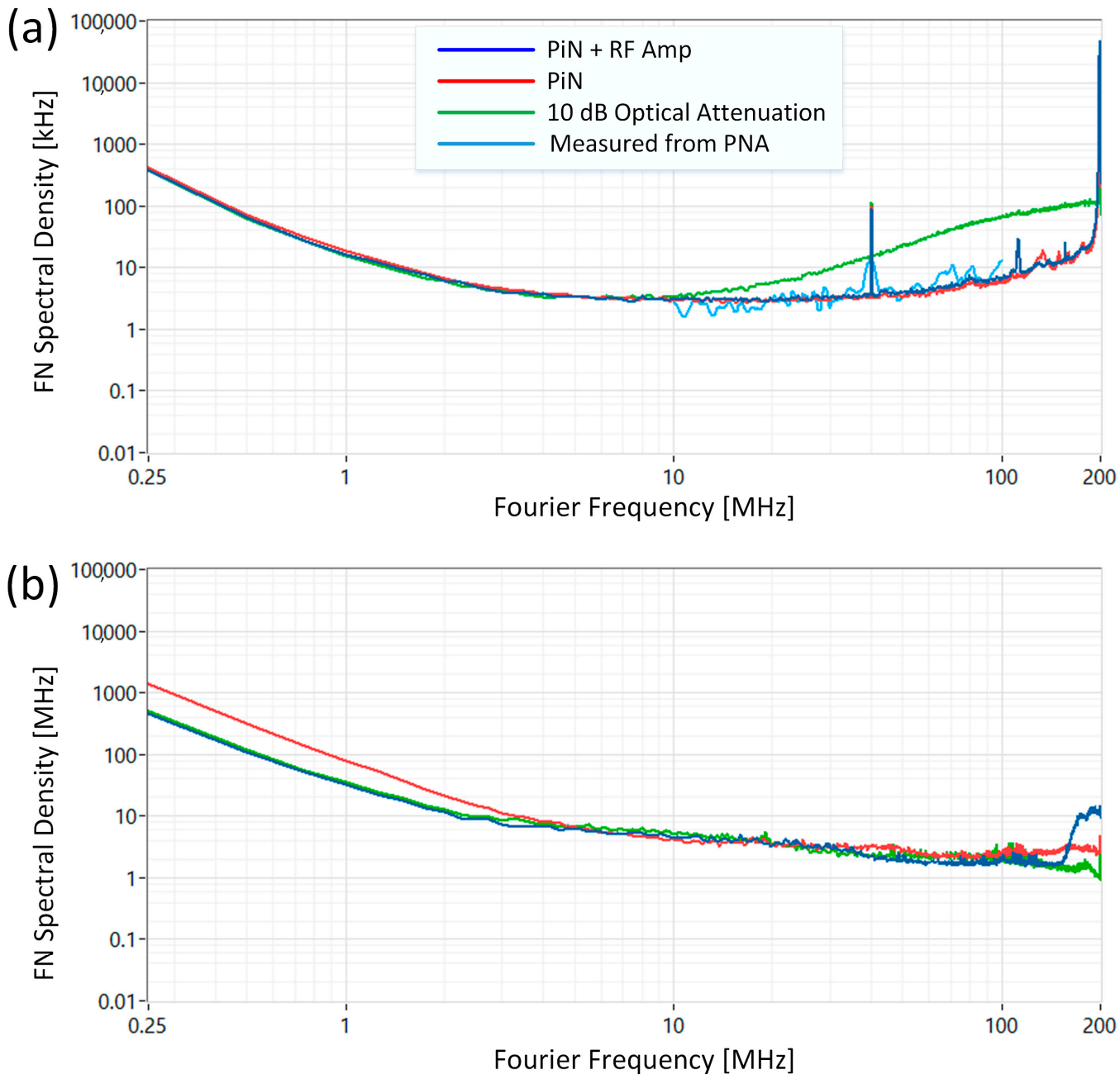

Figure 2. (**a**) Calculated FN spectral density of Laser A and (**b**) calculated FN spectral density of Laser B.

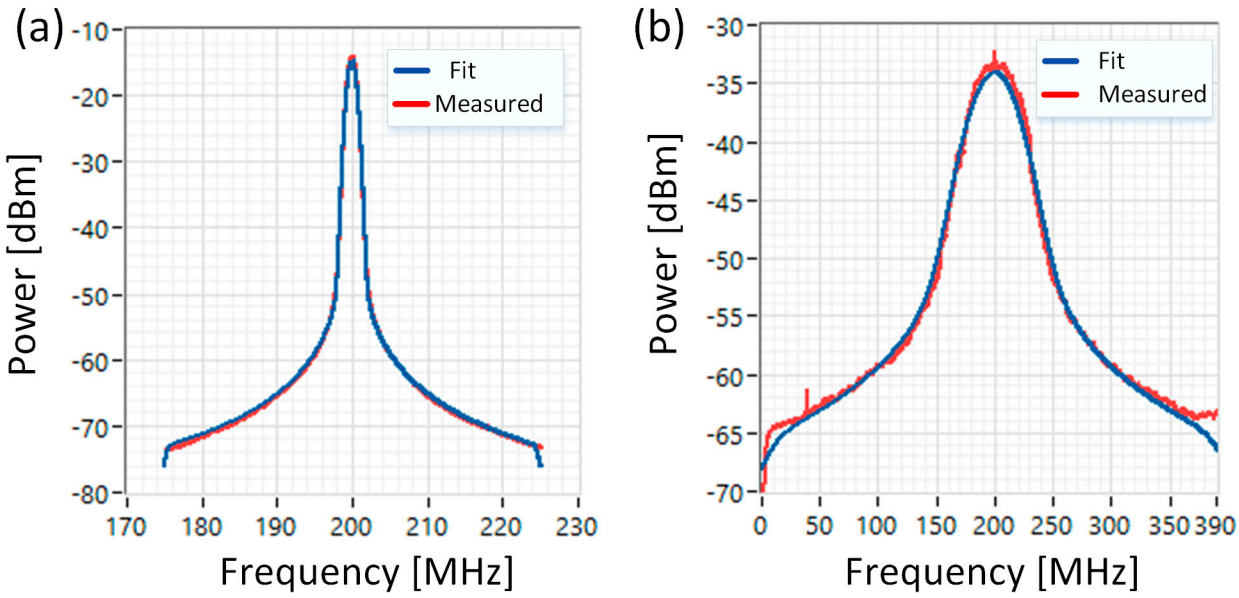

Figure 3. Measured and fitted DSH spectra of (**a**) Laser A, where the intrinsic Lorentzian linewidth was found to be 2.5 kHz and (**b**) Laser B, whose intrinsic Lorentzian linewidth was found to be 2 MHz.

An interesting observation in Figure 2a is the possibility to diagnose spurious tones that appear in the FN spectrum. The spurious tone that appears at 40 MHz and is captured by all three detection scenarios. The source is not the RTO, because the sampling rate is not an integral multiple of 40 MHz, the laser is controlled with an embedded computer system and the culprit is likely to originate from an on-board oscillator; in addition, the PNA trace shown in light blue indicates increased energy over the same spectral range, which points to the source being from the laser side.

The FN results for Laser B are shown in Figure 2b. The intrinsic linewidth of the laser extracted from the FN curves is about 2 MHz. As expected, the case for the PiN + RF Amp and PiN only yielded very similar FN curves, apart from an increase in the $1/f$ FN, which can be attributed to the laser undergoing lower frequency drift when the PiN-only measurement was made. With the 10 dB optical attenuator applied, there is no clear visible noise floor arising from the reduced received power. This was not the case for Laser A with 2.7 kHz linewidth, which has a clearly visible noise floor when the received power was reduced. The DSH spectrum of Laser B is shown in Figure 3b, where the Voigt fit yields an intrinsic Lorentzian linewidth of 2 MHz, which agrees with the FN measurement.

4. Discussion and Conclusions

We have shown and verified a simplified method to measure the frequency noise of CW lasers. The extracted Lorentzian linewidth is similar to that measured from the traditional DSH method with Voight lineshape fitting. The scheme is robust, because one only needs to know the sampling rate of the oscilloscope to calculate the FN. This arises in two places, in calculating the time derivative of the phase in (4) and when using a spectral density estimator [21]. This is in contrast to the PM method, which requires exact knowledge of the f_m to kilohertz accuracy, as well as significant digital processing steps, in order to retrieve the phase noise. The AOM modulating frequency limits the upper Fourier frequency limit that the FN can be measured to; furthermore, AOMs operate at a fixed modulation frequency and are typically available with modulating frequencies of up to a few gigahertz, with the cost increasing monotonically with modulation frequency. If the FN needs to be measured over a wider Fourier frequency range, then the PM method [17] would be preferred because phase modulators with tens of gigahertz of bandwidth are readily available. Despite the complexity, the PM method has also been independently

implemented in [24]. At the time of writing this paper, portable RTOs that meet the sampling requirements of the AOM method exist and would double up as general-purpose laboratory oscilloscopes, whereas bulky, expensive RTOs are needed to meet the tens of gigahertz sampling requirements of the PM method.

The PNA method used to measure the FN is also quite an attractive technique [10,20,25], though it does require a specialized ESA with the PNA tool, and the post-processing requires exact knowledge and/or measurement of the delay between both arms in the interferometer in order to extract the linewidth. The only external information needed for the scheme in this paper to work is knowledge of the RTO sampling rate. The RTO sampling rate is linked to a very precise clock, and one can infer the value from the instrument with confidence.

Another FN measurement scheme exploits a coherent receiver with both arms from the interferometer being fed into the signal and local oscillator ports of an optical hybrid [16,17,26]. The component count in a coherent receiver is substantial, with two sets of balanced photodiodes (per polarization state) being required and two synchronized RTO channels being required to measure the In-phase and Quadrature components of the beating between the two interferometer arms. In the scheme presented here, the In-phase and Quadrature terms are related via the Hilbert transform, thus requiring just a single photodiode and a single RTO channel and digital implementation of the Hilbert transform. Note, the Hilbert transform can be calculated using the FFT [27].

In addition to the FN measurement scheme, we also highlight for the first time the impact that the various components in the receiver have on the FN measurement, especially the use of a PiN without the need for any RF amplification, as well as the importance of receiving the maximum power possible in order to reduce the FN noise floor. This suggests that the laser power is the limiting factor in measuring the FN and has serious consequences, especially when measuring the FN of lasers with very narrow linewidths of a few kilohertz and smaller.

Author Contributions: Conceptualization, S.P.Ó.D.; Methodology, L.P.B.; Software, S.P.Ó.D.; Validation, S.P.Ó.D.; Formal analysis, S.P.Ó.D.; Investigation, L.P.B.; Data curation, S.P.Ó.D.; Writing—original draft, S.P.Ó.D.; Writing—review & editing, L.P.B.; Funding acquisition, L.P.B. All authors have read and agreed to the published version of the manuscript.

Funding: This work was partially supported by Science Foundation Ireland (SFI) through research grants 18/EPSRC/3591 and 12/RC/2276-P2 and by the European Union's HORIZON-EIC-2023-TRANSITION-01 program under grant agreement No. 101137000.

Data Availability Statement: The measurement data of the results contained in this paper are available upon request.

Conflicts of Interest: The authors declare no conflicts of interest.

Appendix A

Here, we provide a computer code that takes the waveform captured with the RTO that produces the FN spectrum. The code provided works for Octave and can be easily adapted into other scientific programming languages. Note that, for some languages, the Hilbert transform operator returns a complex valued signal with the imaginary part being the Hilbert transform of the input array.

The definition of the variables are as follows:

- Waveformis the 1-D array containing the voltage waveform taken from the RTO.
- Rs is the sampling rate of the RTO.
- NFFT is the number of samples considered within each FFT calculation.
- Overlap is the fractional overlap between each subset of waveforms.
- inst_freq is the instantaneous frequency noise extracted from 'waveform' by applying the operators outlined in this paper.
- Pff is the scaled frequency noise spectral density returned by the function.

- freqaxis is the Fourier frequency axis returned by the function.

```
function [Pff, freqaxis] = calc_fn(waveform, NFFT, overlap, Rs)
  waveform = waveform-mean(waveform); # remove DC component, if any
  inst_freq = diff(detrend(unwrap(angle(hilbert(waveform)))))*Rs/2/pi; # the '*' denotes multiplication
  [Pff, freqaxis] = pwelch(inst_freq, [], overlap, NFFT, Rs);
  Pff = Pff*2*pi/2; # scale FN spectral density to be equivalent to linewidth
endfunction
```

References

1. Zhou, Y.; Zheng, C.; Weng, Z.-K.; Inagaki, K.; Kawanishi, T. Effects of a variable linewidth laser and variable linewidth shape laser on coherent FMCW LiDAR. *Opt. Contin.* **2023**, *2*, 1122–1136. [CrossRef]
2. Lee, J.; Hong, J.; Park, K. Frequency Modulation Control of an FMCW LiDAR Using a Frequency-to-Voltage Converter. *Sensors* **2023**, *23*, 4981. [CrossRef] [PubMed]
3. Kazovsky, L. Performance limits and laser linewidth requirements for optical PSK heterodyne communication systems. *IEEE J. Lightwav. Technol.* **1986**, *4*, 415–425. [CrossRef]
4. Taylor, M.G. Phase estimation methods for optical coherent detection using digital signal processing. *IEEE J. Lightwav. Technol.* **2009**, *27*, 901–914. [CrossRef]
5. Savory, S. Digital Coherent Optical Receivers: Algorithms and Subsystems. *IEEE J. Sel. Top. Quantum Electron.* **2010**, *16*, 1164–1179. [CrossRef]
6. Derevianko, M. Accurate and stable timekeeping. *Nat. Rev.* **2019**, *1*, 478–479. [CrossRef]
7. Schawlow, A.L.; Townes, C.H. Infrared and optical masers. *Phys. Rev.* **1958**, *112*, 1940. [CrossRef]
8. McKinstrie, C.J.; Stirling, T.J.; Helmy, A.S. Tutorial on laser linewidths. *Opt. JOSAB* **2021**, *38*, 3837–3848. [CrossRef]
9. Okoshi, T.; Kikuchi, K.; Nakayama, A. Novel method for high resolution measurement of laser output spectrum. *Electron. Lett.* **1980**, *16*, 630–631. [CrossRef]
10. Kikuchi, K.; Okoshi, T. Measurement of FM noise, AM noise, and field spectra of 1.3 pm InGaAsP FP lasers and determination of the linewidth enhancement factor. *IEEE J. Quantum Electron.* **1985**, *21*, 1814–1818. [CrossRef]
11. Morthier, G.; Vankwikelberge, V. *Handbook of Distributed Feedback Laser Diodes*, 2nd ed.; Artech House: Norwood, MA, USA, 2013; ISBN 9781608077021.
12. Ludvigsen, H.; Tossavainen, M.; Kaivola, M. Laser linewidth measurements using self-homodyne detection with short delay. *Opt. Commun.* **1998**, *155*, 180–186. [CrossRef]
13. Tran, M.A.; Huang, D.; Bowers, J.E. Tutorial on narrow linewidth tunable semiconductor lasers using Si/III-V heterogeneous integration. *APL Photonics* **2019**, *4*, 111101. [CrossRef]
14. Chen, M.; Meng, Z.; Wang, J.; Chen, W. Ultra-narrow linewidth measurement based on Voigt profile fitting. *Opt. Express* **2015**, *23*, 6803–6808. [CrossRef] [PubMed]
15. Jain, G.; Andreou, S.; McGuinness, C.; Gutierrez-Pascual, M.D.; Troncoso-Costas, M.; Venkatasubramani, L.N.; Barry, L.P.; Augustin, L.; Smyth, F.; Duggan, S. Widely tunable C-band laser and module with fast tuning and narrow linewidth. *Proc. SPIE* **2023**, *12424*, 339–345.
16. Kikuchi, K. Characterization of semiconductor-laser phase noise and estimation of bit-error rate performance with low-speed offline digital coherent receivers. *Opt. Express* **2012**, *20*, 5291–5302. [CrossRef]
17. Huynh, T.; Nyguyen, L.; Barry, L.P. Delayed self-heterodyne phase noise measurements with coherent phase modulation detection. *IEEE Photonics Technol. Lett.* **2012**, *24*, 249–251. [CrossRef]
18. Dúill, S.P.Ó.; Barry, L.P. High Precision Estimation of Laser FM-Noise Using RF Quadrature Demodulation Techniques. *IEEE Access* **2022**, *10*, 119875–119882. [CrossRef]
19. Brajato, G.; Lundberg, L.; Torres-Company, V.; Karlsson, M.; Zibar, D. Bayesian filtering framework for noise characterization of frequency combs. *Opt. Express* **2020**, *28*, 13949–13964. [CrossRef]
20. Camatel, S.; Ferrero, V. Narrow Linewidth CW Laser Phase Noise Characterization Methods for Coherent Transmission System Applications. *IEEE J. Lightwav. Technol.* **2008**, *26*, 3048–3055. [CrossRef]
21. Welch, P.D. The use of fast Fourier transform for the estimation of power spectra: A method based on time averaging over short modified periodograms. *IEEE Trans. Audio Electroacoust.* **1967**, *15*, 70–73. [CrossRef]
22. Lance, A.L.; Seal, W.D.; Labaar, F. Chapter 7 Phase Noise and AM Noise Measurements in the Frequency Domain. In *Infrared and Millimeter Waves*; Elsevier: Amsterdam, The Netherlands, 1984; Volume 11, eBook, ISBN 9780323152174.
23. Lin, Y.; Dúill, S.P.Ó.; Smyth, F.; Williams, S.; Savchenkov, A.; Barry, L.P. Generation of Spectrally-Efficient Superchannel Using Optical Frequency Comb Referencing and Active Demultiplexing. *arXiv* **2020**, arXiv:1910.00501.
24. McKinzie, K.A.; Wang, C.; Al Noman, A.; Mathine, D.L.; Han, K.; Leaird, D.E.; Hoefler, G.E.; Lal, V.; Kish, F.; Qi, M.; et al. InP high power monolithically integrated widely tunable laser and SOA array for hybrid integration. *Opt. Express* **2021**, *29*, 3490–3502. [CrossRef] [PubMed]
25. Llopis, O.; Bailly, G.; Bougaud, A.; Fernandez, A. Experimental investigations on lasers FM and AM noise. In Proceedings of the Joint Conference of the IEEE International Frequency Control Symposium and International Symposium on Applications of Ferroelectrics (IFCS-ISAF), Keystone, CO, USA, 19–23 July 2020. [CrossRef]

26. Lei, F.; Ye, Z.; Helgason, Ó.B.; Fülöp, A.; Girardi, M.; Torres-Company, V. Optical linewidth of soliton microcombs. *Nat. Commun.* **2022**, *13*, 3161. [CrossRef] [PubMed]
27. Bracewell, R.N. *The Fourier Transform & Its Applications*; McGraw Hill: New York, NY, USA, 1999; ISBN 978-0071160438.